# Stable Structures of Neutral and Charged Iron Clusters by Self-Consistent Tight-Binding Molecular-Dynamics

*Materials Transactions, JIM*, Vol. 40, No. 9 (1999), pp. 859 to 862
*Papers from JIM Spring Meeting (1999)*

# Stable Structures of Neutral and Charged Iron Clusters by Self-Consistent Tight-Binding Molecular-Dynamics†

Akito Taneda and Yoshiyuki Kawazoe

*Institute for Materials Research, Tohoku University, Sendai 980-8577, Japan*

By using the simulated-annealing technique with a tight-binding molecular-dynamics, fully optimized structures of iron clusters are determined for the number of atoms, $n$=2–17. It is found that the clusters with sizes, $n$=6, 7, and 13, are relatively stable. Iron clusters show an icosahedral growth similar to rare gas clusters. HOMO-LUMO energy gaps are calculated, and electronic shell effects are absent. Additionally, by performing a self-consistent tight-binding molecular-dynamics calculations, we obtain fully optimized structures of positively- and negatively-charged iron clusters. Nearest-neighbor distance of positively- and negatively-charged iron clusters reveals an decrement and increment compared to that of the neutral clusters, respectively. These changes in the interatomic distances are mainly due to the changes in the number of HOMO electrons in anti-bonding molecular-orbitals.

(Received May 6, 1999; In Final Form June 16, 1999)

***Keywords***: *simulated-anneling, geometric shell effects, icosahedral growth, interatomic distances, electronic density of states*

## I. Introduction

The study of physical properties of transition metal clusters is an increasingly active area of research. Although many theoretical and experimental efforts have been made in this field, determination of stable structures and the physical properties of charged transition metal clusters still have been subjects of research. Iron clusters are one of the intensively studied transition metal clusters; iron clusters have many interesting features, *e.g.*, enhanced magnetic moments[1] and magic number clusters[2]. To understand such physical properties, it is important to find out the stable structures of the clusters. Usually first-principles molecular-dynamics calculations are performed to determine the stable structures of clusters. Although this approach is accurate and reliable, it is quite time-consuming. For this reason, the largest structure optimization has ever been done by first-principles molecular-dynamics is limited to a simulated-annealing calculation of $Fe_7$ by Ballone and Jones[3].

In the present paper, we carry out a tight-binding molecular-dynamics (TB) calculation to determine the stable structures of iron clusters. This method can estimate interatomic forces on the basis of electronic structures, and is much more efficient compared to first-principles calculations. We apply TB to determine the stable structures of neutral $Fe_2$–$Fe_{17}$ clusters. Using these obtained stable structures for neutral clusters as an initial configuration, we perform a self-consistent tight-binding molecular-dynamics (SCTB) so as to optimize the structures of neutral and charged iron clusters in the same size region. By comparing the results from these calculations, we discuss the charging effects on interatomic distances and electronic density of states.

## II. Computational Method

TB parameters we use have functional forms proposed by Mehl and Papaconstantopoulos[4]-[6]. As a basis set, orthogonal spd basis set is adopted. We determine the TB parameters by fitting to the first-principles results from FLAPW calculation (package code, WIEN95[8]), in which data from non-magnetic bcc and fcc irons are included. To efficiently optimize the structures of the clusters, we use both TB and SCTB. First, we perform simulated-annealing (SA) calculations for neutral clusters with TB. In TB, total-energy is expressed as,

$$E_{\mathrm{tot}}^{\mathrm{TB}}=\sum_{\lambda}^{\mathrm{occ.}}\varepsilon_{\lambda}f_{\lambda}, \tag{1}$$

where, $\lambda$ is index for eigenstate, $\varepsilon_{\lambda}$ eigenvalue, and $f_{\lambda}$ occupation number of electrons[4]. By differentiating eq. (1) with respect to atomic positions, interatomic forces are derived analytically. To find out a global minimum in a phase space of $3n$ dimension (where $n$ is the number of atoms), SA technique is adopted[7]. Annealing of clusters are performed with a TB code specifically parallelized for HITACHI SR2201 parallel computer and started from 16 random initial configurations at each cluster size.

In the second step of the structure optimization, we carry out the structure relaxation with SCTB. In this step, the stable structures are determined for neutral and positively- and negatively-charged iron clusters. Initial configurations for the structure relaxation are taken from the results from TB. In SCTB, total-energy has an expression,

† This Paper was Presented at the Spring Meeting of the Japan Institute of Metals, held in Tokyo, on March 30, 1999.

†† Graduate Student, Tohoku University.

$$E_{\mathrm{tot}}^{\mathrm{SCTB}}=\sum_{\lambda}^{\mathrm{occ.}}\sum_{i,j}f_{\lambda}C_i^{\lambda *}H_{ij}^{\mathrm{TB}}C_j^{\lambda}+\frac{1}{2}\sum_{\alpha,\beta}\Delta q_{\alpha}\Delta q_{\beta}\gamma_{\alpha\beta},$$

$$\Delta q_{\alpha}=q_{\alpha}-q_{\alpha}^{0},\quad \gamma_{\alpha\beta}=\frac{1}{\sqrt{R_{\alpha\beta}^{2}+\frac{1}{4}\left(\frac{1}{U_{\alpha}}+\frac{1}{U_{\beta}}\right)^{2}}}, \qquad (2)$$

where, $C_i^{\lambda *}$, $C_j^{\lambda}$ are elements of eigenvector, $H_{ij}^{\mathrm{TB}}$ is a Hamiltonian matrix element in TB, $q_{\alpha}$, $q_{\alpha}^{0}$ are electronic charges on site $\alpha$ and isolated neutral atom, $R_{\alpha\beta}$ is a interatomic distance between site $\alpha$ and $\beta$, and $U_{\alpha}$ is the Hubbard parameter of atom $\alpha$[9]. In SCTB, charge transfer effects are approximately included by point charges on each atomic nuclear positions. $\gamma_{\alpha\beta}$ becomes equal to the Hubbard parameter at $R_{\alpha\beta}=0$, which corresponds to the Coulomb repulsion between the electrons located in the same atom. On the other hand, $\gamma_{\alpha\beta}$ becomes the Coulomb potential at $R_{\alpha\beta}\to\infty$. Hence $\gamma_{\alpha\beta}$ continuously interpolates these two limits. We can obtain the total-energy in SCTB by solving eq. (2) self-consistently. Equation (2) can be differentiated with respect to atomic positions, hence interatomic forces in SCTB can also analytically be given. In both TB and SCTB, atomic positions are updated by the velocity Verlet algorithm, in which 1 MD time step is taken as 1 fs.

## III. Results and Discussion

**Figure 1** shows obtained stable structures of $Fe_3$–$Fe_{17}$. It is seen from Fig. 1 that $Fe_3$ is a triangle and $Fe_4$ has a tetrahedral shape. $Fe_5$ is a bitetrahedron, $Fe_6$ a bipyramid structure, and $Fe_7$ has a structure with a pentagonal symmetry. In $Fe_3$–$Fe_7$, our results agree well with the results from the pseudopotential calculation by Ballone and Jones[3]; though Ballone and Jones obtained tricapped tetrahedron as the most stable structure for $Fe_6$, energy difference between tricapped tetrahedron and bipyramid is only about 0.02 eV/atom†. Since this difference is very small, as Ballone and Jones mentioned, these two structures almost degenerate[3]. $Fe_8$ consists of $Fe_7$ and one adatom, and then iron clsuters show a growth to icosahedral $Fe_{13}$ by addition of adatoms. $Fe_{14}$–$Fe_{17}$ also show a growth on the basis of an icosahedral regime.

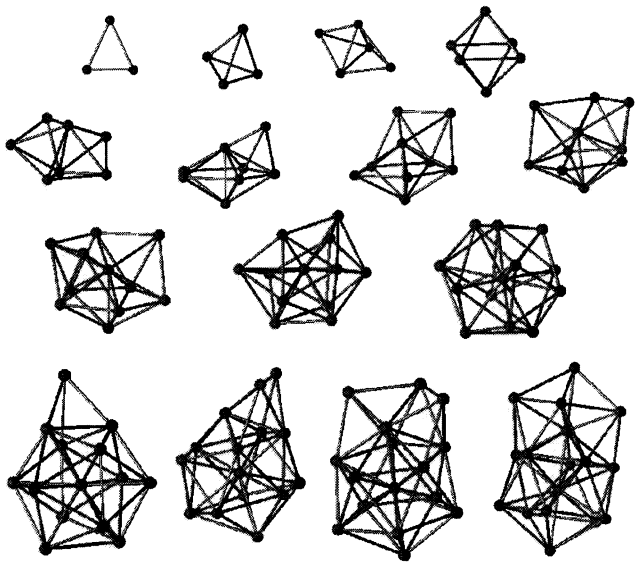

Fig. 1 Stable structures of $Fe_n$ ($n$=3–17).

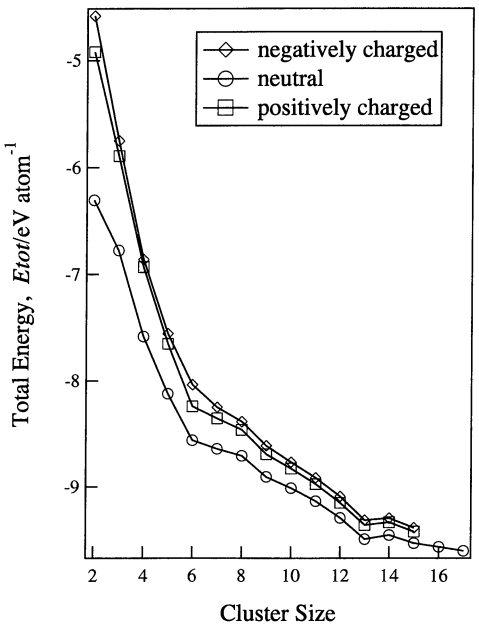


Fig. 2 Cluster size dependence of total-energy of iron clusters.

In **Fig. 2**, a cluster size dependence is shown for the total-energy of neutral and positively- and negatively-charged iron clsuters. From the figure, it is obvious that $Fe_6$, $Fe_7$ and $Fe_{13}$ are relatively stable compared to the others. Generally, stable clusters at the ground state are due to geometric or electronic shell effects. For instance, geometric shell effects cause magic numbers of rare gas clusters, and electronic shell effects are related to magic number clusters of alkali and coinage metal clusters. In the present study, the cluster size dependence of the total-energy of charged clusters is similar to that of neutral clusters. These results indicate that the stability of iron clusters are not so affected by the total number of electrons, hence we can say that the electronic shell effects are not found in the total-energy curve for $Fe_2$–$Fe_{17}$. In **Fig. 3**, a cluster size dependence of HOMO-LUMO energy gap is shown. From the figure, we cannot see any specifically large gaps at size $n$=6, 7, and 13, where also electronic shell effects cannot be seen. From these results and the fact that $Fe_6$, $Fe_7$, and $Fe_{13}$ have geometrically closed structure, we conclude that the extraordinary stability in iron clusters with $n$=6, 7, and 13 are ascribed to geometric shell effects.

**Figure 4** shows a cluster size dependence of the nearest-neighbor distances of neutral and charged iron clusters. Since cluster has usually many defferent nearest-neighbor distances, their averaged values are adopted as the nearest-neighbor distances in the present

† 1 eV ≈ $1.6\times10^{-19}$ J, 1 eV·atom$^{-1}$ ≈ $9.65\times10^{4}$ J·mol$^{-1}$.

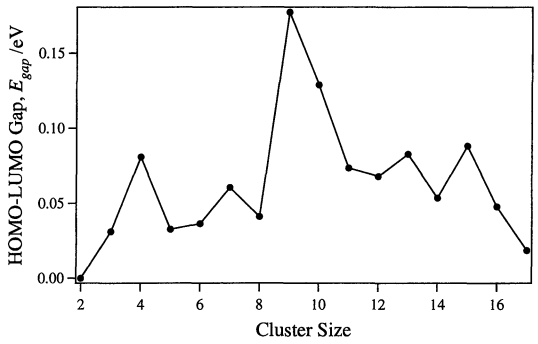


Fig. 3 Cluster size dependence of HOMO-LUMO energy gap of iron clusters.

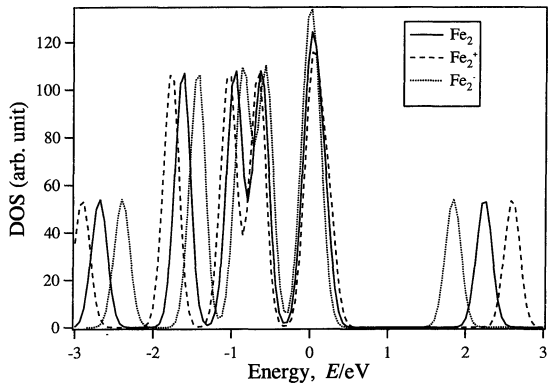


Fig. 5 Electronic density of states for $Fe_2$, $Fe_2^+$, and $Fe_2^-$. Fermi-energy is set to zero.

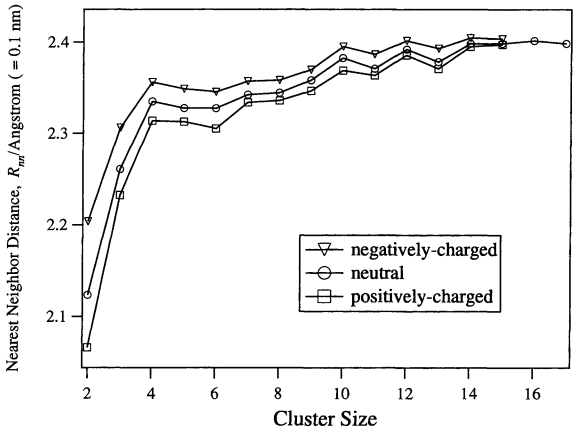


Fig. 4 Cluster size dependence of nearest-neighbor distance of iron clusters.

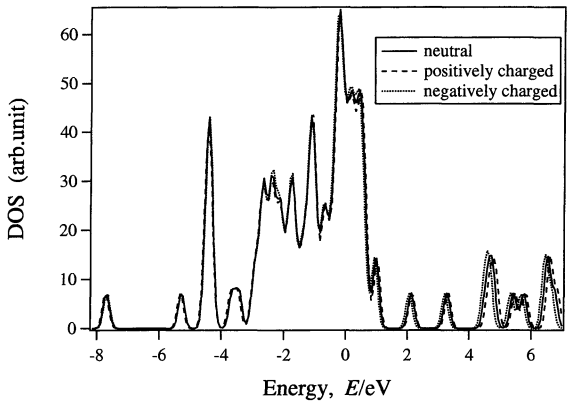


Fig. 6 Electronic density of states for $Fe_{15}$, $Fe_{15}^+$ and $Fe_{15}^-$. Fermi-energy is set to zero.

paper. As can be seen from Fig. 4, compared to neutral clusters, the nearest-neighbor distances decrease and increase in positively- and negatively-charged clusters, respectively. From the figure, it is also recognized that $Fe_2$ has the largest change (about 3%), and the charging effects become negligible at $Fe_{15}$. These changes in interatomic distance can qualitatively be understood by the concept of the molecular-orbitals (MOs). In cluster, the MOs are classified into bonding orbitals and anti-bonding orbitals. Iron atom has 6 d-electrons, and an iron atom in a cluster has also about 6 d-electrons as valence electrons. Since the number of d-orbitals is 5 per atom, if we assume that the half of MOs belong to bonding orbitals and the another half belong to anti-bonding orbitals, the number of bonding orbitals is $5n/2$, where $n$ is the number of atoms. Considering spin degree of freedom, we have, (the total number of d-electrons) $-$ (the number of bonding d-electrons) $= 6n - 5n = n$. Hence $Fe_n$ has $n$ d-electrons in anti-bonding orbitals. As a result, when the number of anti-bonding electrons decreases (positively-charged state), bonding becomes stronger, and this leads to decrement of nearest-neighbor distance. On the other hand, if the number of anti-bonding electrons increases (negatively-charged state), bonding become weaker, and this causes increment of nearest-neighbor distance. **Figure 5** shows electronic DOS for $Fe_2$, $Fe_2^+$, and $Fe_2^-$. The width of electronic DOS for $Fe_2^+$ and $Fe_2^-$ reveals increment and decrement compared to that for $Fe_2$, respectively, which correspond to contraction and expansion of the clusters. In the case of $Fe_{15}$, as shown in **Fig. 6**, only a little difference between the charged and neutral clusters is found. These results indicate that the charging effects on the electronic structure are negligible at $Fe_{15}$ and for larger clusters.

## IV. Summary

By performing SA with TB and SCTB, we determined the stable structures of neutral and charged iron clusters. Iron clusters show growth according to icosahedral regime similar to rare gas clusters. As the specifically stable clusters, $Fe_6$, $Fe_7$, and $Fe_{13}$ are obtained. These results are due to geometric shell effects. Charging effects appear as changes in the interatomic distances and the electronic density of states, and these effects almost vanish at $Fe_{15}$.

*Acknowledgments*

The authors are grateful for the Materials Information Science Group of the Institute for Materials Research, Tohoku University, for their continuous support of the supercomputing facilities.

## REFERENCES

(1) I. M. L. Billas, A. Chatelain and W. A. Heer: Science, **265** (1994), 1682–1684.
(2) M. Sakurai, K. Watanabe, K. Sumiyama and K. Suzuki: J. Phys. Soc. Jpn., **67** (1998), 2571–2573.
(3) P. Ballone and R. O. Jones: J. Chem. Phys., **233** (1995), 632–638.
(4) M. J. Mehl and D. A. Papaconstantopoulos: Phys. Rev., **B54** (1996), 4519–4530.
(5) C. Barreteau, D. Spanjaard and M. C. Desjonqueres: Phys. Rev., **B58** (1998), 9721–9731.
(6) For spin-polarized version, see A. Taneda and Y. Kawazoe: J. Magn. Soc. Japan, **23** (1999), 679–681.
(7) A. Taneda, K. Esfarjani, Y. Hashi and Y. Kawazoe: *Similarities and Differences between Atomic Nuclei and Clusters*, Ed. Y. Abe, I. Arai, S. M. Lee and K. Yabana, The American Institute of Physics, (1998), p. 471–474.
(8) P. Blaha, K. Schwarz, P. Dufek and R. Augustyn: Technical University of Vienna, 1995. [Improved and updated UNIX version of the original copyrighted WIEN-code, which was published by P. Blaha, K. Schwarz, P. Sorantin and S. B. Trickey, Comput. Phys. Commun., **59** (1990), 399–415.]
(9) Th. Frauenheim, D. Porezag, M. Elstner, G. Jungnickel, J. Elsner, M. Haugk, A. Sieck and G. Seifert: *Tight-Binding Approach to Computational Materials Science*, Ed. P. E. A. Turchi, A. Gonis and L. Colombo, (Mater. Res. Soc. Symp. Proc. vol. 491, Boston, 1998), p. 91–104.